Available online at www.sciencedirect.com

ScienceDirect

journal homepage: http://www.elsevier.com/locate/acme

Original Research Article

Mechanical and microstructural aspects of C20-steel blades subjected to gas nitriding

Barbara Kucharska [a,*], *Jerzy Michalski* [b], *Grzegorz Wójcik* [a]

[a] *Czestochowa University of Technology, Faculty of Production Engineering and Materials Technology, 19 Armii Krajowej Street, 42-200 Czestochowa, Poland*

[b] *Institute of Precision Mechanics, 3 Duchnicka Street, 01-796 Warszawa, Poland*

ARTICLE INFO

Article history:
Received 14 May 2018
Accepted 20 September 2018
Available online 17 October 2018

Keywords:
Gas nitriding
Through-nitriding
Conical blades
C20 steel

ABSTRACT

The paper presents the investigation of conical blades made of unalloyed steel C20 gas-nitrided by the Nitreg method. On the surface of steel blades (with tip angles in the range of 20–170°) an approx. 15 mm-thick nitride layer of was fabricated, which had a bizonal structure of: ε ($Fe_{2-3}N$ and $Fe_3(N,C)_{1-x}$) and ε + γ′(Fe_4N) with a hardness of 1310 HV and 910 HV, respectively. Hardness tests carried out on blade cross-section showed that a 0.7–1 mm thick diffusion layer occurred under the nitride layer. By applying the criterion of effective nitrided layer thickness, g_{c+50}, it was demonstrated that blades with a tip angle of 20° and 30° had been through-nitrided (i.e. nitrided through and through). A static compression test showed that, as a result of nitriding, the compressive strength of the blades had increased by a factor of two.

© 2018 Politechnika Wrocławska. Published by Elsevier B.V. All rights reserved.

1. Introduction

Hardening the surface of steel by thermochemical methods, including nitriding, is applied wherever high tribological and mechanical properties of the surface are required. Nitriding enables steel hardness to be increased even up to 1500 HV, whereby nitriding of machine parts and tools is commonly used in the machine-building, automotive, aircraft, aerospace and arms industries [1]. Among the most commonly nitrided parts are shafts, bushing, gear wheels, coupling parts, spindles, drawing dies, cutting tools, drills, and even shells.

Nitriding processes can be carried out in gas media using the Nitreg of the Zero Flow methods and under reduced pressure conditions (LPN) [2]. The Nitreg nitriding method has been developed in the Institute of Precision Mechanics in Warsaw and is currently used in many industrial plants both home and abroad. For the control of the nitriding process, this method makes use of the nitrogen potential (N_p), which is defined as the ratio of ammonia-to-hydrogen partial pressures in the nitriding atmosphere, $N_p = p_{NH_3}/p_{H_2}^{3/2}$ [3]. The structure of the nitride layer, in particular the surface layer of nitrides, depends on the values of the nitrogen potential and temperature, according to the Lehrer diagram [4].

Gas nitriding, at a temperature in the range of 480–600 °C, is applied to unalloyed and alloyed constructional steels [5]. The source of nitrogen in those processes is ammonia (NH_3). Under the process conditions, ammonia absorbed on the surface of

* *Corresponding author.*
E-mail addresses: kucharska.barbara@wip.pcz.pl (B. Kucharska), michalski@imp.edu.pl (J. Michalski), wojcik.grzegorz@wip.pcz.pl (G. Wójcik).

https://doi.org/10.1016/j.acme.2018.09.006
1644-9665/© 2018 Politechnika Wrocławska. Published by Elsevier B.V. All rights reserved.

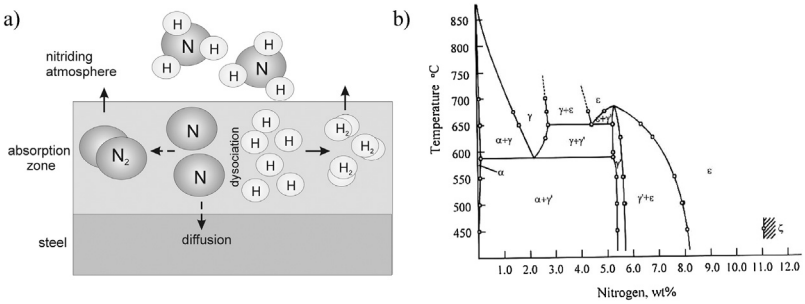

Fig. 1 – (a) Schematic diagram of the nitriding process and (b) the Fe-N phase diagram.

steel being treated undergoes gradual dissociation, and thus formed atomic nitrogen diffuses into the steel (Fig. 1a).

Regardless of the nitriding method, the size and the shape of the nitrided product, the nitrided layer forms on all surfaces that are reached by the nitriding atmosphere and can be subjected to further, additional surface treatments [6,7].

The phase composition of the nitrided layer formed on iron is consistent with the Fe-N phase equilibrium diagram (Fig. 1b). According to the diagram, high-nitrogen phases, such as nitrides of type ε-$Fe_{2-3}N$ (approx. 8–11 wt%) of a hexagonal structure, including a nitride defined as ζ-Fe_2N, form in the outer zone of the layer. The next zone in the layer is made up of a mixture of nitrides ε and γ′. Nitrides γ′ of a regular structure exhibit stoichiometry of type Fe_4N (Fig. 2).

The layer built of nitrides ε-$Fe_{2-3}N$ (in the case of carbon steels, carbonitride $Fe_2(C,N)_{1-x}$ often forms) and γ′-Fe_4N makes up the outer zone of the whole nitrided layer, which is known as the iron nitride surface layer (white layer). In the inner zone under the iron nitride layer, a solution layer occurs, which is called the inner nitriding layer. It is built of nitrogen-saturated ferrite with precipitates of nitrides γ′ (α(N) + γ′), while deeper on, solely of nitrogen ferrite – α(N) [8].

The structure and thickness of the produced nitride layer determine the operational durability of nitrided products. For example, the surface layer of iron nitrides enhances the abrasion resistance, while reducing the resistance to dynamic loads. Nitrides γ′ have lower hardness and better plastic properties, compared to ε nitrides; thus, the overall mechanical resistance of a layer built of a mixture of both nitrides is better.

Generally, the nitrided layer is described by stating its surface hardness, the thickness of the surface iron nitride later (and possibly its phase composition) and the effective thickness of the inner nitriding zone. The effective thickness is determined based on the hardness criterion, g_{c+l}, where c is the steel core hardness and l is the declared increase in hardness, compared to the core [9]. This parameter is significant in the case of alloy steels; for unalloyed steels, it is of no significant importance.

Depending on the nitriding process parameters and the grade of nitrided steel, nitrided layers of a varying structure can be obtained, in which the following three groups can be distinguished [10]:

- Group I – layers with a 17–25 μm-thick surface iron nitride layer, which are made up of a α(N) solution zone and an Fe_4N iron nitride layer (γ′ phase), a mixture of (ε + γ′) phases and, on the surface, a porous Fe_3N nitride zone (ε phase). Nitrided constructional alloy and unalloyed steels have a porous zone 6–12 μm in depth. Such layers are recommended for parts operating under friction conditions. After impregnation with the Econcorr DW-T preparation with a corrosion inhibitor, they provide very good corrosion protection [11].
- Group II – nitrided layers with a surface iron nitride layer of a thickness of up to 13 μm. The layers are composed of an α(N) solution zone and an Fe_4N nitride layer (γ′ phase) or a mixture of the ε and γ′ phases, and are used for machine parts and tools of alloy steel, which are exposed to abrasive wear under high loads [12].
- Group III – nitrided layers with no surface iron nitride layer, made up only of an α(N) solution layer. These layers are used for machine parts and tools operating under dynamic and impact loads. They are fabricated exclusively on alloy steels [13].

The present study has undertaken investigation into an unalloyed steel subjected to gas nitriding, done also through-

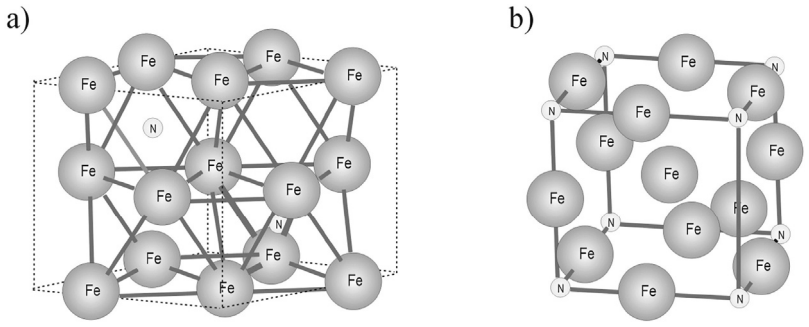

Fig. 2 – The crystal structure of nitrides: (a) ε-$Fe_{2-3}N$ (P−31m) and (b) γ′-Fe_4N (Pm−3m).

out the product (i.e. through-nitriding), on the example of conical blades. Blades of different divergence angles are used as the punches and reamers to make holes in plastics, wood and thin metal sheets and tapes. An example of industrial applications is, for instance, the manufacture of anti-skidding platforms and graters for domestic appliances.

2. Material and research methodology

The subject of investigation was steel blades in the form of cones. The blades were made from a Ø10 mm bar of steel C20 (AISI 1020), and had the following sequence of tip angles: 20°, 30°, 45°, 60°, 90°, 120°, 140° and 170°. The chemical composition of steel C20 is given in Table 1, while a general view and the dimensions of the blades are shown in Fig. 3.

The quality of execution of the cones, that is their ''sharpening'' with an employed machining method, was evaluated by the observation of their tips using a scanning microscope (JEOL JSM-6610LV) at a magnification of 150× (Fig. 4). Thus determined diameters of blade tips were contained in the range of 50–400 μm (Table 2).

Table 1 – Chemical composition of the C20 steel (acc. to ISO 683/18-1996) used for making the blades (wt%).

C	Mn	Si	P	S
0.17–0.23	0.3–0.6	max. 0.1	≤0.04	≤0.05

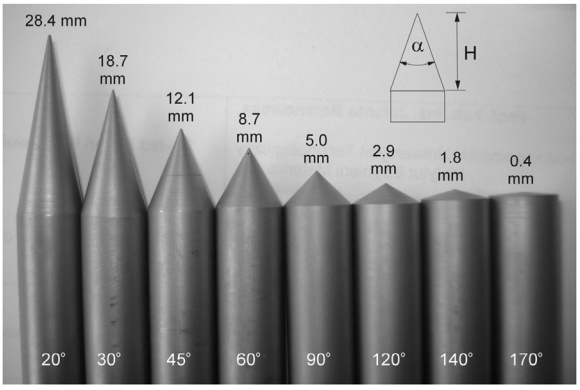

Fig. 3 – A general view of varying-tip angle blades made for the investigation.

Table 2 – Diameters of the tips of the blades investigated.

Tip angle	20°	30°	45°	60°	90°	120°	140°	170°
Tip diameter (μm)	400	242	240	200	50	100	110	300

The blades were subjected to gas nitriding at the parameters of the process allowed nitrided layers of Group I to be obtained on the steel. The steady-state temperature was 570 °C for a duration of 4 h. The nitrogen potential assumed values from the ε phase stability region throughout the process. At the steady-state temperature, its average value was 2.5 $atm^{-0.5}$ (Fig. 5).

The examinations of the microstructure and nitrided layer thickness were made on the longitudinal sections of the blades, from which microsections were prepared. The microstructures of nitride layers were recorded using a light microscope (Axiovert 25) and a scanning microscope (Phenom World). On etched longitudinal sections, the hardness of the iron nitride layer (white layer) was also measured with a Berkovich indenter (an NHT Anton Paar nano-hardness tester) under a load of 10 mN and by the Vickers method under a load of 0.5 N. The distribution of hardness within the blades at a varying distance from their tips was determined. The duration of making indentations was 10 s.

The phase composition of the layers was examined by the X-ray diffractometry method using the radiation of $K_\alpha Co = 0.17902$ nm (a Seifert 300TT diffractometer) in the tip angle range of 25–120°.

The mechanical resistance of nitrided layers on the blades was evaluated in an experiment involving static, perpendicular pressing of the blades into the hardened C20 steel of a hardness of 756 HV0.05. Blades of an overall length of approx. 17 mm were subjected to pressure until the cross-beam of a testing machine (Zwick Roell Z100) had travelled by 1.5 mm.

3. Investigation results

3.1. *Structure of nitrided layers*

The phase composition of the nitrided layers was examined on rolled fragments of specimens. Sample diffraction patterns are shown in Fig. 6. They show that the nitrided layers were built primarily of ε-$Fe_{2-3}N$ nitrides and a smaller quantity of γ′-Fe_4N nitrides, with their respective volumetric fractions being 80%

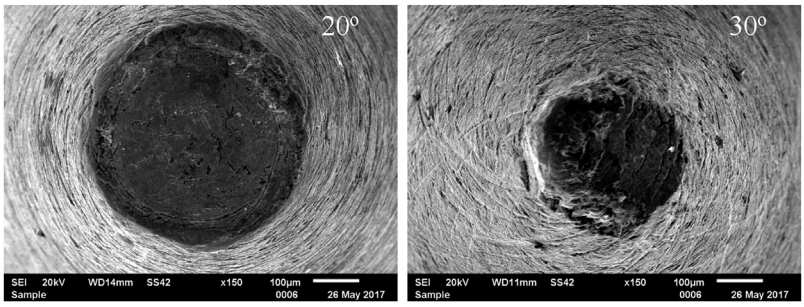

Fig. 4 – Top view of conical blade tips with a tip angle of 20° and 30°, respectively.

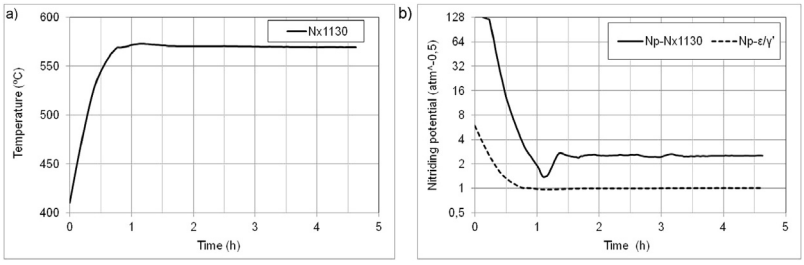

Fig. 5 – Parameters of the gas nitriding process: (a) temperature and (b) nitrogen potential (Np-Nx1130 – actual nitrogen potential value; Np-ε/γ′ – potential value corresponding to the ε/γ′ interface).

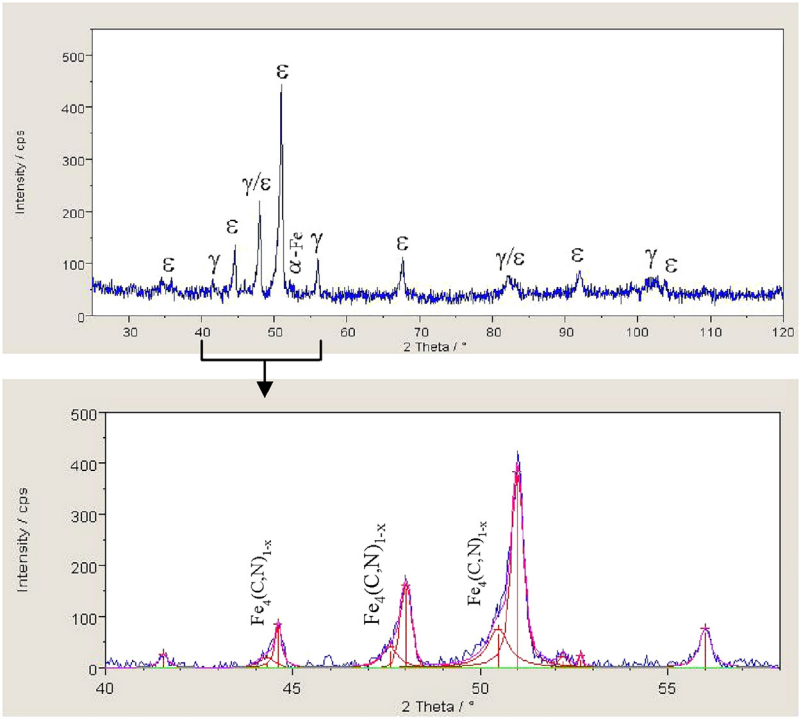

Fig. 6 – A diffraction pattern of a nitrided layer on C20 steel bar surface.

and 20%. The asymmetric profile of diffraction reflections associated with ε nitrides indicates that part of them formed based on the iron carbide ($Fe_3(N,C)_{1-x}$) that occurs in pearlite. It should be also emphasized that the asymmetric profile of reflections may also be influenced by the curvature of the examined blade surface. A very weak reflection coming from the steel substrate was recorded in the diffraction patterns, which means that the average thickness of the nitride layer (white nitride layer) is slightly less than 15 μm, as this is the maximum iron nitride thickness allowing reflections from the steel substrate to be recorded using $K_\alpha Co$ radiation.

Layer thickness measurements taken on the cross-sections of rolled specimen parts by the microscopic method confirmed the nitrided layer thickness estimated in X-ray measurements. In turn, the layer thicknesses shown on the longitudinal sections of conical blades in the vicinity of their tips differed slightly in the range of 10–35 μm (Fig. 7). This was caused by difficulty in making the sections and then their grinding exactly through the cone tip.

The white layer on the steel cones had a bizonal structure, which was porous in the outer zone (30–40% of the white layer thickness) and solid in the zone at the substrate (Fig. 8). Moreover, observations of the layer at the ferritic-pearlitic substrate showed that nitrides formed faster on pearlite insulae. It can be supposed that the nitrides nucleated preferentially on cementite (Fe_3C) lamellas, and these nitrides could have a larger lattice parameter expressed by an asymmetry of diffraction reflections from ε nitrides towards smaller diffraction angles.

3.2. *Hardness of nitride layers*

The microstructure of the nitride layer (so-called white layer), in the non-porous zone at the substrate, was diphase (Fig. 9).

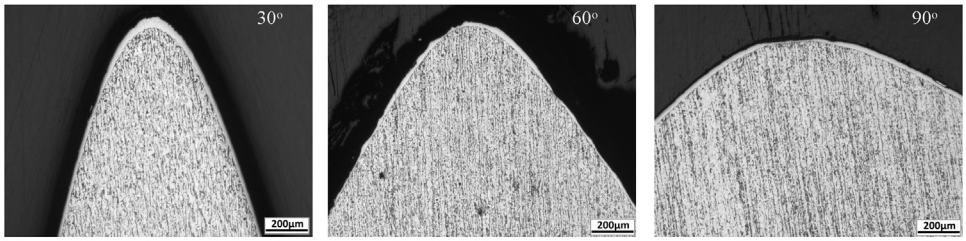

Fig. 7 – Longitudinal sections of steel cones in the region of their tips.

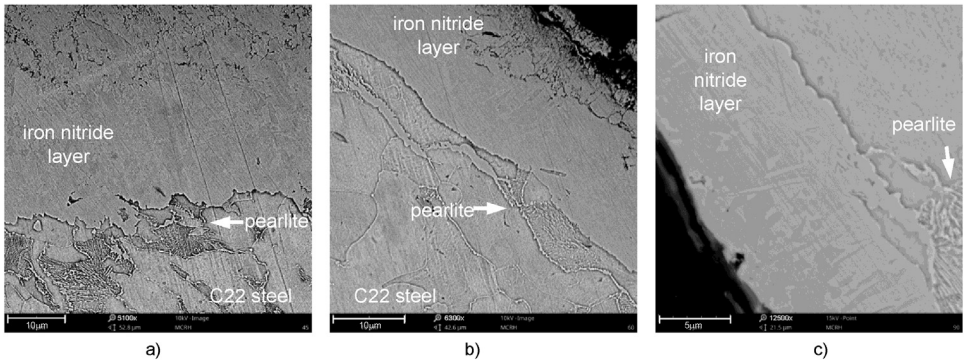

Fig. 8 – Microstructures of nitride layers on the conical blade surfaces: (a) 45°, (b) 60° and (c) 90°.

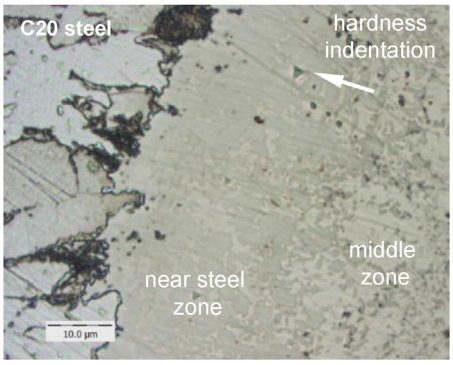

Fig. 9 – Microstructure of the iron nitride layer in the zone at the steel substrate with a sample hardness test indentation (a 45° blade).

The zone visible on the microstructure as the lighter one (middle zone) are ε nitrides, whose volumetric fraction decreased in favour of the darker γ′ nitride phase towards the substrate (near steel zone). The determination of the hardness of both zones was made on the longitudinal section of conical blades of a tip angle of 45°, 60° and 90°. The hardness test results (Berkovich indenter), as converted into Vickers hardness units, are given in Table 3.

3.3. *Hardness of steel cones*

Hardness was measured on the sections of cones with a tip angle of 20° and 30°. The hardness measurements were taken on longitudinal cone sections in the direction perpendicular to the axis at a distance from the tip of 90 µm, 180 µm, 900 µm and 10 mm, respectively (Fig. 10). Fig. 10 shows the determined hardness distributions, where the extreme measurements were taken in the nitride later (white layer).

The average iron nitride hardness, as determined in different locations on the longitudinal cone section under a load of 0.5 N, was 652 HV0.05 and 706 HV0.05, respectively, for 20° and 30°-angle blades. The hardness values were smaller than those obtained from nano-hardness tester measurements, given in Table 3. This is due to the different measurement method, and also to the specificity of the conical surface section. Namely, under the surface subjected to the indenter action, the material volume was smaller, compared to the measurements taken closer to the cone axis. Under a bigger load, the material would therefore show a lower resistance to the indenter action, so thus determined hardness of the layers was less than the actual one. The impact of this practical difficulty in taking measurements on the section of conical parts (also rolled and spherical ones) on the determined hardness was reflected in the hardness determined on the white layer on the 20° cone, which was less by approx. 50 HV0.05 than the hardness of the white layer on the 30° cone. The selection of the 0.5 N load for the determination of the hardness distributions, which was smaller than the one used as standard for measurements on nitrided layer, was therefore

Table 3 – Hardness of phases in the nitride layer.

Layer on the blade	Middle zone – ε nitrides	Near steel zone – ε + γ′ nitrides
45°	1312	951
60°	1304	904
90°	1320	878
HV_{av}	1312	911

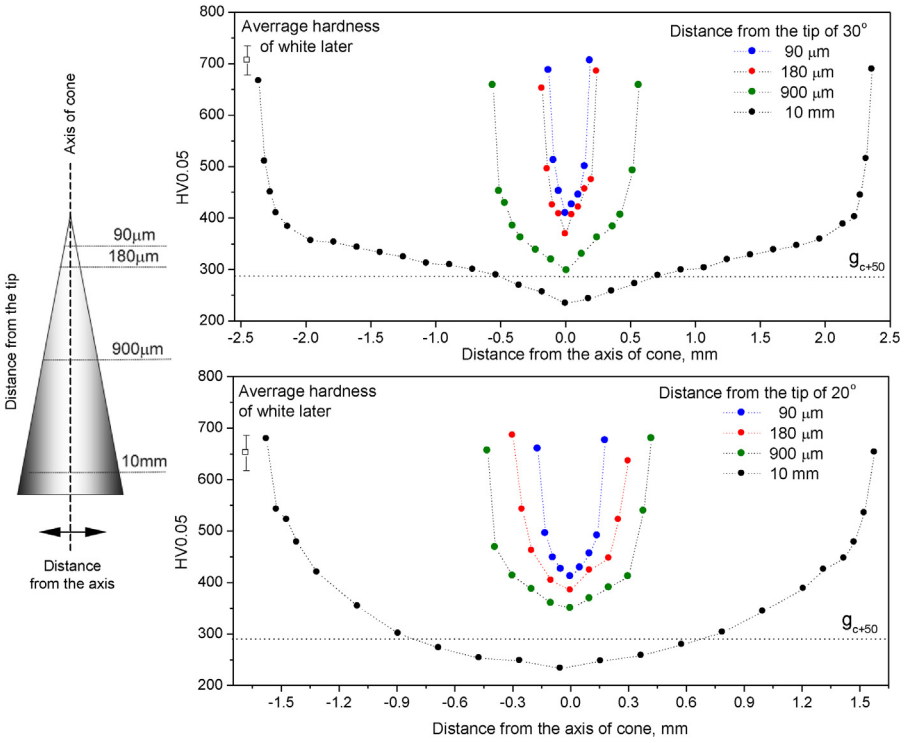

Fig. 10 – Hardness (HV0.05) measurement scheme and hardness distribution on the sections of cones at a varying distance from the tip. The hardness of the white layer is defined only by the extreme measurement points (the most distant from the axis of the cones). The average value of white layer hardness of all extreme points is denoted by the symbol □.

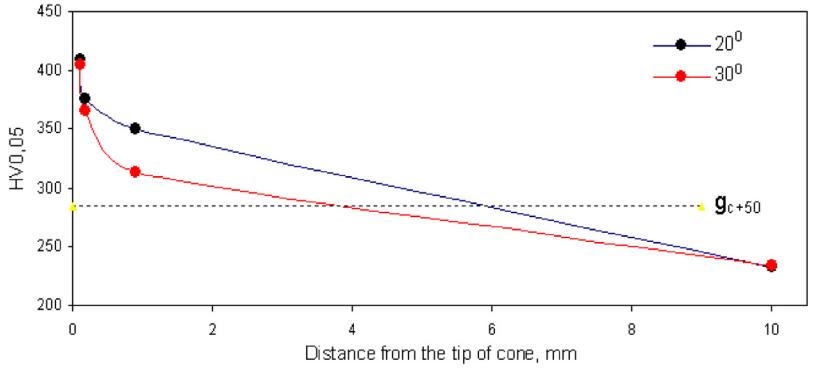

Fig. 11 – Hardness in the axis of nitrided cones at varying distances from the top.

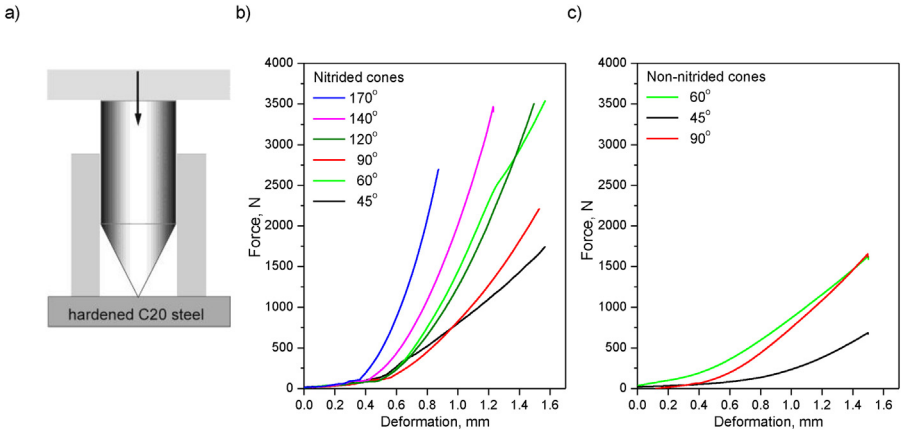

Fig. 12 – (a) Schematic diagram of the blade compression test and the loading curves for (b) nitrided and (c) non-nitrided blades.

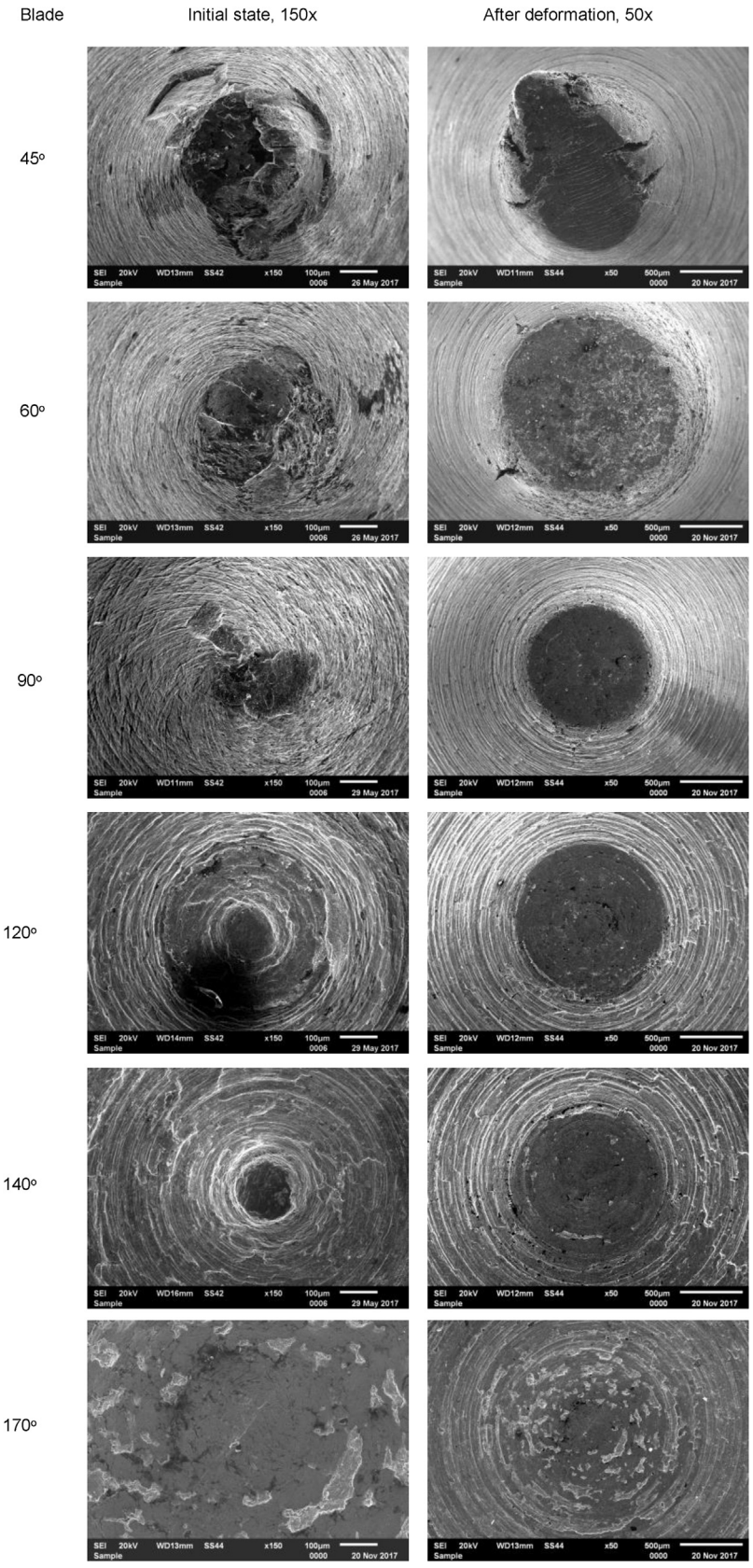

Fig. 13 – Blade tips before and after the compression test.

a trade-off between the correctly determined hardness and the accurate representation of its variation within the blade.

The analysis of the hardness distributions in Fig. 10 shows that, in spite of the distinct interface between the nitride layer and the steel substrate, a nitrogen-saturated zone occurs in the steel. In the specimens tested, the width of that zone was estimated at 0.7–1 mm. At a distance of 10 mm from the tips of the investigated conical blades, approx. 1/2 (in the 20°-angle blade) and approx. 1/4 (in the 30°-angle blade) of their section have a hardness lower than resulting from the criterion of effective thickness, g_{c+50}, that is 284 HV0.05. The width of that steel region not hardened by nitriding decreased with decreasing distance from the tip, until a state was attained, in which the hardness on the entire cone blade section was greater than 284 HV0.05, which means that the blade was nitrided through and through (i.e. through-nitrided). Based on the graph illustrating cone axis hardness at a varying distance from the tip (Fig. 11) it was estimated that the 20°-angle blade was through-nitrided up to approx. 6 mm from the tip, while the 30°-angle blade, up to approx. 4 mm from the tip.

3.4. *Compressive strength of conical blades*

Blade specimens were pressed into a 10 mm-thick hardened C20 steel plate. The specimens were put in a sleeve and then compressed with an initial force of 100 N using a testing machine until their heights had been reduced by 0.9–1.5 mm (Fig. 12).

Compressive forces were the smallest for the blade of a tip angle of 45° and increased with increasing specimen tip angles. Compared to non-nitrided blades, their compressive strength

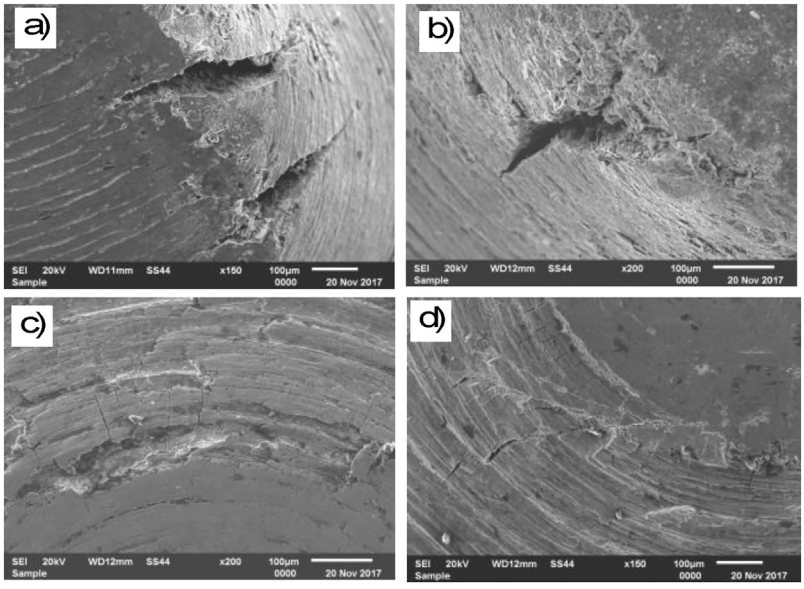

Fig. 14 – Cracks within the region of a blade tip with a tip angle of (a) 45°, (b) 60°, (c) 120° and (d) 140°.

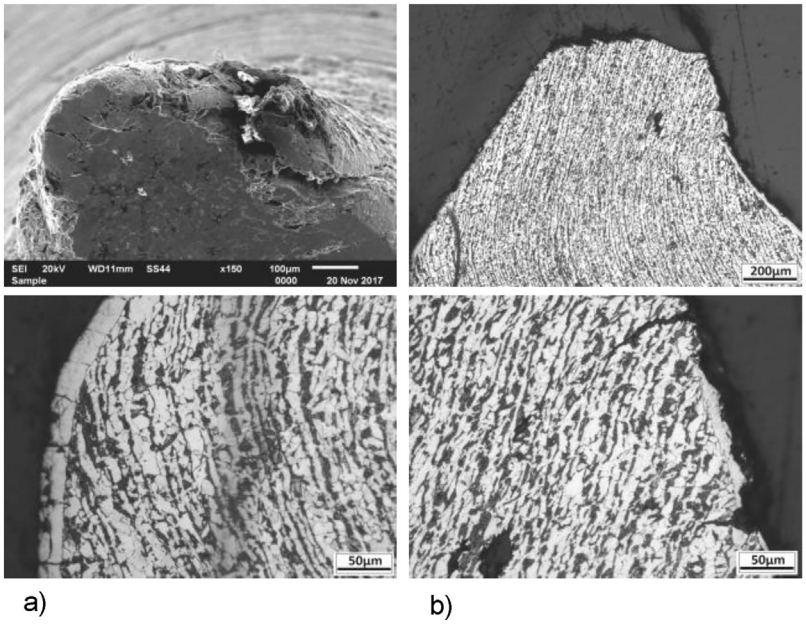

Fig. 15 – The condition of a nitride layer on a 45° blade after the compression test: (a) SEM and (b–d) longitudinal section.

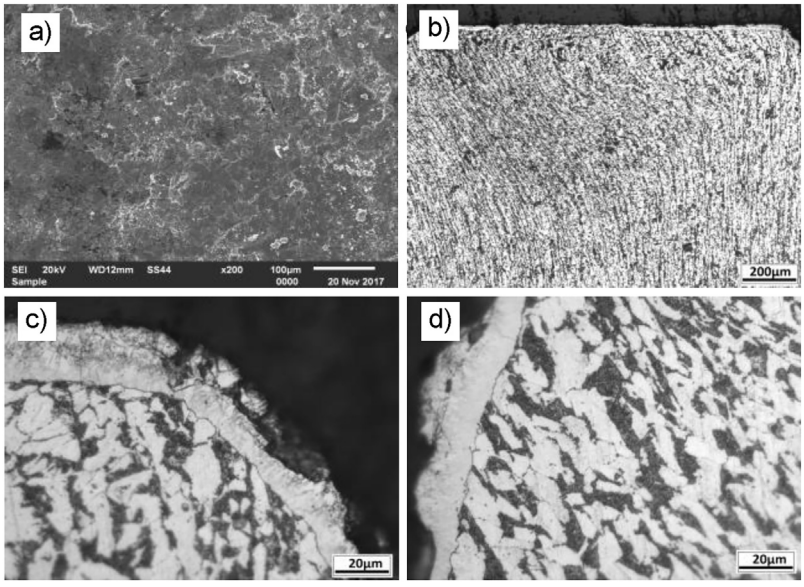

Fig. 16 – The condition of a nitride layer on a 60° blade after the compression test: (a) SEM and (b–d) longitudinal section.

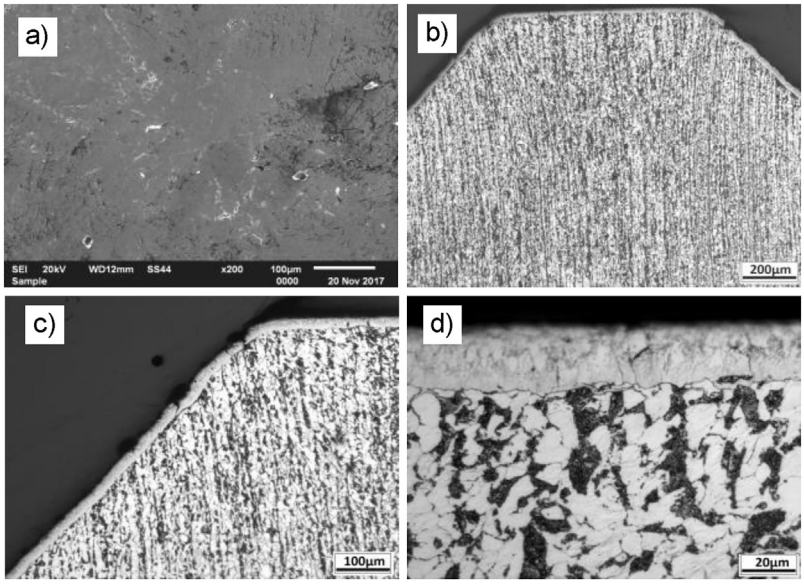

Fig. 17 – The condition of a nitride layer on a 90° blade after the compression test: (a) SEM and (b–d) longitudinal section.

increased twofold. The compression test of blades with larger tip angles (140° and 170°) was ended at a deformation smaller than 1.5 mm due to the shorter conical part of the specimens. After compression, blade tips were examined for the condition of the steel and the nitride layer (Fig. 13).

On all blades, except for the 170° blade, cracks occurred. The deepest cracks into the steel occurred on the 45° and 60° blades (Fig. 14). On the other blades, the crack depth decreased steadily with increasing tip angles, and cracks occurred only within the nitride layer (Figs. 15–17). Moreover, the smallest-angle blade tips were sheared, as a result of which their surfaces after compression were not completely flat and perpendicular to the axis.

4. Conclusions

The investigation of the microstructure and properties of conical blades of ferritic-pearlitic steel C20 subjected to gas nitriding has found the following:

- during 4 h of nitriding at a temperature of 570 °C, an approx. 15 μm-thick iron nitride layer forms on steel C20, which is built of nitrides ε and γ′ with their respective volumetric fractions of the entire layer amounting to 80% and 20%. The outer, porous ε nitride zone of a hardness of 1300 HV accounts for 30–40% of the layer thickness. The layer zone

near the substrate is built of a mixture of ε and γ′ nitrides and exhibits a hardness less than 900 HV;
- iron carbides in pearlite are a preferred place for nitride nucleation in the steel, as a result of which part of the phase is made up by carbonitrides of type $Fe_3(C,N)_{1-x}$;
- in spite of a distinct phase boundary between the nitride layer and the steel substrate, a 0.7–1 mm-wide diffusion zone occurs in the steel (as determined according to the g_{c+50} criterion), through the agency of which blades of tip angles of 20°and 30° were through-nitrided over a length of, respectively, 6 and 4 mm;
- nitrided blades exhibit compressive strength two times as high as that of non-nitrided blades.

Funding body

Czestochowa University of Technology.

REFERENCES

[1] L. Małdziński, Thermodynamic, kinetic and technological aspects of the producing nitrided layers on iron and steel in processes of gas nitriding, Ed. Technical University of Poznan, 2002 (in Polish).
[2] P. Wach, J. Michalski, J. Tacikowski, S. Kowalski, M. Betiuk, Gas nitriding and its variants in industrial application, Inż. Mater.-Mater. Eng. 6 (166) (2008) 808–811 (in Polish).
[3] L. Maldzinski, W. Liliental, G. Tymowski, J. Tacikowski, New possibilities for controlling gas nitriding process by simulation of growth kinetics of nitride layer, Surf. Eng. 15 (5) (1999) 377–384.
[4] E. Lehrer, Über das Eisen-Wasserstoff-Ammoniak Gleichgewicht, Z. Elektrochem. 36 (6) (1930) 383–392.
[5] J. Ratajski, R. Olik, Development of nitrided layer during nitriding of steel, Adv. Mater. Res. 83–86 (2010) 1025–1034.
[6] K. Dybowski, Ł. Kaczmarek, E. Pietrasik, J. Smolik, Ł. Kołodziejczyk, D. Baroty, M. Gzik, M. Stegliński, Influence of chemical heat treatment on the mechanical properties of paper knife-edge die, J. Achiev. Mater. Manuf. Eng. 37 (2) (2009) 422–427.
[7] M. Kulka, D. Panfil, J. Michalski, Modelling of the effects of laser modification of gas-nitrided layer, Arch. Mater. Sci. Eng. 2 (88) (2017) 59–67.
[8] J. Smolik, J. Walkowicz, J. Tacikowski, Influence of the structure of the composite: nitrided layer/PVD coating on the durability of tools for hot-working, Surf. Coat. Technol. 125 (2000) 134–140.
[9] M. Betiuk, J. Michalski, J. Tacikowski, Z. Łataś, Measuring of the thickness of iron nitrides layers, Inż. Powierzchni 2 (2014) 60–66.
[10] Norma AMS 2759/10A, Automated gaseous nitriding controlled by nitriding potential.
[11] J. Michalski, J. Iwanow, J. Tacikowski, I. Sułkowski, P. Wach, T. N. Tarfa, J. Tymowski, Anti-corrosion nitriding, with post-oxidation and inhibitor impregnation, and its industrial applications, Heat Treat. Met. 31 (2) (2004) 31–35.
[12] J. Michalski, P. Wach, K. Burdyński, M. Betiuk, Control and regulation of the kinetics of layer thickness increase in controlled gas nitriding processes, Inż. Powierzchni 2 (2015) 34–40 (in Polish).
[13] J. Michalski, J. Tacikowski, P. Wach, J. Ratajski, Controlled gas nitriding of 40HM and 38HMJ steel grades with the formation of nitrided cases with and without the surface compound layer, composed of iron nitride, J. Mech. Constr. Maintenance, Problemy Eksploatacji 2 (2006) 43–51.